

# A reduced model for fingering instability in miscible displacement

Irina Brailovsky<sup>a</sup>, Alexander Babchin<sup>b</sup>, Michael Frankel<sup>c</sup>, Gregory Sivashinsky<sup>a,\*</sup>

<sup>a</sup> School of Mathematical Sciences, Tel Aviv University, Tel Aviv 69978, Israel

<sup>b</sup> Heavy Oil and Oil Sands, Alberta Research Council, Edmonton, AL T6N1E4, Canada

<sup>c</sup> Department of Mathematical Sciences, Indiana University Purdue, University, Indianapolis, IN 46202-3216, USA

Received 16 January 2007; received in revised form 17 April 2007; accepted 18 April 2007

Available online 29 April 2007

Communicated by C.R. Doering

## Abstract

The classical problem of fingering instability in miscible displacement is revisited. The finger-forming dynamics is considered as a multiple-scale process involving a thin inter-diffusion layer and large-scale background flow affected by the viscosity and/or density stratification. Upon an appropriate separation of ‘fast’ and ‘slow’ variables one ends up with a reduced model dealing directly with the evolving displacement front. As an illustration, the new model is applied for description of fingering in a source-supported flow and in a flow within a vertical channel.

© 2007 Elsevier B.V. All rights reserved.

PACS: 47.20.Bp; 47.20.Gv; 47.20.Ky; 47.20.Ma

Keywords: Fingering instability; Displacement fronts; Surface dynamics

## 1. Introduction

In oil recovery technology it is common practice to inject a solvent into the oil field at certain spots in an attempt to drive oil to certain other spots for pumping. In this process, if the solvent is less viscous than the oil, the phenomenon of fingering has long been identified. The solvent, which is intended to push the oil forward, tends to penetrate the oil through spontaneously formed multi-branched channels (fingers). As a result, the advancing displacement front assumes a highly corrugated coral-like configuration [1–3]. A morphologically different kind of fingering (meandering worms) occurs in superimposed miscible fluids, provided the upper fluid is heavier [4].

Since the solvent and the oil are miscible there is no surface tension separating the fluids. As a result the displacement front widens continuously due to the solvent-oil inter-diffusion, rendering the basic concentration profile time dependent. The

unsteadiness of the profile is a major complicating factor in the theoretical exploration of the problem. Most of the previous work on the subject therefore adopted the so-called quasi-steady-state approximation (QSSA) which assumes the growth rate of disturbances to be much faster than the rate of change of the basic state [5–8]. Although QSSA captures some of the salient features of the system quite successfully [9], it runs into difficulty in the long-wavelength limit where the growth rate of disturbances vanishes, thereby violating the basic premise of the QSSA. In the present Letter we consider the opposite limit where the spatio-temporal structure of the disturbances is assumed to be slowly-varying compared to that of the inter-diffusion layer. The asymptotic separation of spatio-temporal variables then leads to a compact reduced model dealing directly with the displacement front and its finger-forming dynamics.

## 2. Formulation

Assuming that the porous medium is homogeneous with a constant permeability  $K$ , the flow  $\mathbf{u}$  is incompressible, the diffusivity  $D$  is isotropic, the governing equations may be writ-

\* Corresponding author.

E-mail addresses: [brailir@post.tau.ac.il](mailto:brailir@post.tau.ac.il) (I. Brailovsky), [babchin@arc.ab.ca](mailto:babchin@arc.ab.ca) (A. Babchin), [mfrankel@math.iupui.edu](mailto:mfrankel@math.iupui.edu) (M. Frankel), [grishas@post.tau.ac.il](mailto:grishas@post.tau.ac.il) (G. Sivashinsky).

ten as

$$\nabla \cdot \mathbf{u} = 0, \quad (1)$$

$$\nabla P = -(\mu(c)/K)\mathbf{u} + \rho(c)\mathbf{g}, \quad (2)$$

$$c_t + \mathbf{u} \cdot \nabla c = D\nabla^2 c. \quad (3)$$

Eqs. (1), (2) are the continuity equation and Darcy's law, while Eq. (3) is the diffusion equation for the solvent concentration  $c$ ;  $\mathbf{g}$  is the gravity vector. The concentration is set at unity far behind the displacement front and at zero far ahead. The front is identified with the iso-concentration interface,  $c = 1/2$ . It is further assumed that the relationships between the viscosity  $\mu$ , density  $\rho$  and concentration  $c$  are known. For simplicity of the further analysis, yet without much detriment to general understanding, the discussion is restricted to stepwise dependencies (see also Section 9),

$$\begin{aligned} \mu &= \mu_a, & \rho &= \rho_a & \text{at } 0 < c < 1/2, \\ \mu &= \mu_b, & \rho &= \rho_b & \text{at } 1/2 < c < 1. \end{aligned} \quad (4)$$

The subscripts  $a$ ,  $b$  mean *ahead* and *behind* the displacement front ( $c = 1/2$ ). The ratio  $\lambda = K/\mu$  is referred to as the mobility of the system.

### 3. Intrinsic geometry and front-attached coordinates

In order to make the analysis tractable the diffusion equation (3) will be written in front-attached Bertrand intrinsic coordinates, instantaneously normal and parallel to the displacement front. Details of the transformation between Cartesian and Bertrand coordinates may be found in Refs. [10–12]. For brevity, we restrict the discussion to two dimensions. In the extension to three dimensions the curvature  $\mathcal{K}$  which appears in the theory is the sum of the principal curvatures.

The Bertrand coordinates  $(s, n)$  are related to the Cartesian coordinates  $\mathbf{r} = (x, y)$  by the change of variables given by

$$\mathbf{r} = \mathbf{R}(s, t) + n\mathbf{N}(s, t), \quad (5)$$

where  $\mathbf{R}(s, t)$  is the evolving interface.  $\mathbf{N}(s, t)$  is the unit normal to the interface directed towards the fluid ahead of the interface.  $s$  is the arclength measured along the interface, and  $n$  is the distance from the interface.

In the intrinsic coordinates the flow velocity may be written as

$$\mathbf{u} = u_s \mathbf{T} + u_n \mathbf{N}, \quad (6)$$

where  $\mathbf{T} = \partial \mathbf{R} / \partial s$  is the unit tangent vector to the interface. The continuity (1) and diffusion (3) equations then become

$$\frac{\partial u_n}{\partial n} + \frac{\mathcal{K}u_n}{1+n\mathcal{K}} + \frac{1}{1+n\mathcal{K}} \frac{\partial u_s}{\partial s} = 0, \quad (7)$$

$$\begin{aligned} \left( \frac{\partial c}{\partial t} \right)_n - V_n \frac{\partial c}{\partial n} + \frac{u_s}{1+n\mathcal{K}} \frac{\partial c}{\partial s} + u_n \frac{\partial c}{\partial n} \\ = \frac{\partial^2 c}{\partial n^2} + \frac{\mathcal{K}}{1+n\mathcal{K}} \frac{\partial c}{\partial n} + \frac{1}{1+n\mathcal{K}} \frac{\partial}{\partial s} \left( \frac{1}{1+n\mathcal{K}} \frac{\partial c}{\partial s} \right). \end{aligned} \quad (8)$$

Here  $\mathcal{K} = \nabla \cdot \mathbf{N}$  is the curvature of the interface,  $V_n = \partial \mathbf{R} / \partial t \cdot \mathbf{N}$  is its normal velocity.  $(\partial c / \partial t)_n$  is the intrinsic time derivative

along the normal  $\mathbf{N}$ . There is a simple connection between the intrinsic time derivative and partial time derivative at constant  $s$  [10],

$$\left( \frac{\partial c}{\partial t} \right)_n = \frac{\partial c}{\partial t} + V_s \frac{\partial c}{\partial s}, \quad (9)$$

where  $V_s$  is the arclength rate of stretch,

$$V_s = \left( \frac{\partial s}{\partial t} \right)_n = \int_0^s \mathcal{K} V_n d\hat{s}. \quad (10)$$

For the total arclength  $L$  of the evolving interface Eq. (10) yields

$$\frac{dL}{dt} = \int_0^L \mathcal{K} V_n d\hat{s}. \quad (11)$$

### 4. Scaling and asymptotic analysis

Assume that at  $t = 0$  the concentration profile is given by the step-function,

$$c(n < 0) = 1, \quad c(n > 0) = 0, \quad (12)$$

and the interface is weakly curved,

$$\mathcal{K} \sim \varepsilon, \quad \varepsilon \ll 1. \quad (13)$$

Then, one may expect that at  $t > 0$  the spatio-temporal structure of the developing solution will involve short-range variables  $n$ ,  $t$ , associated with the widening inter-diffusion layer, and long-range variables  $\varepsilon n$ ,  $\varepsilon \xi$ ,  $\varepsilon t$ , associated with the curved interface and flow-field away from the interface.

Since at  $\varepsilon n \sim 1$  the concentration is expected to be exponentially close to the initial profile (12) one may exclude  $\varepsilon n$  from its spatial variables. Thus,

$$c = c(n, t, \varepsilon s, \varepsilon t). \quad (14)$$

For stepwise dependencies (4) the hydrodynamic field is not directly affected by the processes within the diffusion layer, and one therefore may exclude  $n, t$  from its variables. Thus,

$$\mathbf{u} = \mathbf{u}(\varepsilon n, \varepsilon s, \varepsilon t). \quad (15)$$

The prior removal of certain variables allows to somewhat reduce algebraic manipulations (see also Section 9).

In terms of the scaled variables,

$$\kappa = \mathcal{K}/\varepsilon, \quad \xi = \varepsilon s, \quad \eta = \varepsilon n, \quad \tau = \varepsilon t. \quad (16)$$

Eqs. (7), (8), applied to the diffusive layer ( $n \sim 1$ ), yield

$$\begin{aligned} \frac{\partial c}{\partial t} + (\bar{u}_n - V_n - \varepsilon \kappa D) \frac{\partial c}{\partial n} + \varepsilon \frac{\partial c}{\partial \tau} + \varepsilon (V_s + \bar{u}_s) \frac{\partial c}{\partial \xi} \\ - \varepsilon n \frac{\partial \bar{u}_s}{\partial \xi} \frac{\partial c}{\partial n} - \varepsilon n \kappa \bar{u}_n \frac{\partial c}{\partial n} = D \frac{\partial^2 c}{\partial n^2} + O(\varepsilon^2). \end{aligned} \quad (17)$$

Here  $\bar{u}_n = u_n(\eta = 0)$ ,  $\bar{u}_s = u_s(\eta = 0)$ .

For the zeroth-order approximation Eq. (17) yields

$$c^{(0)} = \frac{1}{2} - \frac{1}{2} \operatorname{erf} \left( \frac{n - (\bar{u}_n - V_n^{(0)})t}{2\sqrt{Dt}} \right), \quad (18)$$

which meets the boundary conditions at  $n = \pm\infty$ . The condition  $c^{(0)}(n=0) = 1/2$  (Section 2) then readily implies

$$V_n^{(0)} = \bar{u}_n, \quad (19)$$

$$c^{(0)} = \frac{1}{2} - \frac{1}{2} \operatorname{erf}\left(\frac{n}{2\sqrt{Dt}}\right). \quad (20)$$

Thus,  $c^{(0)}$  does not involve the long-range variables  $\xi$  and  $\tau$ . That is,  $\varepsilon c_\tau = O(\varepsilon^2)$  and  $\varepsilon c_\xi = O(\varepsilon^2)$ . As a result, for the first-order approximation,  $c = c^{(0)} + \varepsilon c^{(1)} + O(\varepsilon^2)$ , Eq. (17) may be written as

$$\begin{aligned} \frac{\partial c}{\partial t} + (\bar{u}_n - V_n - \varepsilon D\kappa) \frac{\partial c}{\partial n} - \varepsilon \left( \frac{\partial \bar{u}_s}{\partial \xi} + \kappa \bar{u}_b \right) n \frac{\partial c}{\partial n} \\ = D \frac{\partial^2 c}{\partial n^2} + O(\varepsilon^2). \end{aligned} \quad (21)$$

The term  $\varepsilon n \partial c / \partial n = \varepsilon n \partial c^{(0)} / \partial n + O(\varepsilon^2)$  is an odd function which does not affect the solution at  $n = 0$ . Hence, the condition  $c(n=0) = 1/2$  applied to the relevant solution of Eq. (21) yields

$$V_n = \bar{u}_n - \varepsilon D\kappa = \bar{u}_n - DK. \quad (22)$$

The curvature term  $DK$  provides dissipation of the short-wavelength disturbances, thereby ensuring well-posedness of the associated initial value problem. Eq. (22) effectively replaces the diffusion equation (3). Being considered jointly with Eqs. (1), (2) and (4), Eq. (22) reduces the problem of miscible displacement to a free-interface problem.

## 5. Evaluation of $\bar{u}_n$

By virtue of Darcy's law (2) and conditions (4) the pressure beyond the interface is described by the Laplace equation,

$$\nabla^2 P = 0, \quad (23)$$

which should be considered jointly with the jump conditions on the interface,

$$[\nabla P \cdot \mathbf{N}]_b^a = -J(s, t), \quad (24)$$

$$[P]_b^a = 0, \quad (25)$$

where

$$\begin{aligned} J = (\lambda_a^{-1} - \lambda_b^{-1}) \bar{u}_n - (\rho_a - \rho_b) g_n, \\ g_n = \mathbf{g} \cdot \mathbf{N}, \quad \lambda = K/\mu. \end{aligned} \quad (26)$$

A further analysis of the system may therefore be conducted in the framework of the classical theory of the Newtonian or logarithmic potentials [13], allowing to connect the shape of the interface with the normal velocity  $\bar{u}_n$  appearing in Eq. (22). In this Letter, the discussion is restricted to two geometrical situations: (i) the displacement front as a closed curve  $\mathcal{L}$  evolving through a two-dimensional zero-gravity flow sustained by a point-source of a prescribed intensity  $Q$ ,

$$\mathbf{g} = 0, \quad \mathbf{u} = \frac{Q}{2\pi} \frac{\mathbf{r}}{|\mathbf{r}|^2} \quad \text{at } \mathbf{r} \rightarrow 0, \quad (27)$$

and (ii) displacement in a vertical channel ( $0 < x < \ell$ ,  $-\infty < y < \infty$ ) with periodic boundary conditions at the walls,

$$\mathbf{g} = (0, -g), \quad \mathbf{u}(x, \pm\infty, t) = \mathbf{u}_\infty = (0, u_\infty). \quad (28)$$

For the source case (i),

$$P = \frac{Q}{2\pi\lambda_b} \ln \frac{1}{|\mathbf{r}|} + \frac{1}{2\pi} \int_{\mathcal{L}} JG(\mathbf{r} - \hat{\mathbf{r}}) d\mathcal{L}_{\hat{\mathbf{r}}}, \quad (29)$$

where

$$G = -\ln |\mathbf{r} - \hat{\mathbf{r}}|. \quad (30)$$

On the  $b$ -side of the interface,

$$\begin{aligned} \left( \frac{dP}{dn} \right)_b = -\frac{Q}{2\pi\lambda_b} \frac{\mathbf{r} \cdot \mathbf{N}}{|\mathbf{r}|^2} + \frac{1}{2} \left( \frac{1}{\lambda_a} - \frac{1}{\lambda_b} \right) \bar{u}_n(\mathbf{r}, t) \\ - \frac{1}{2\pi} \left( \frac{1}{\lambda_a} - \frac{1}{\lambda_b} \right) \int_{\mathcal{L}} \frac{\bar{u}_n(\hat{\mathbf{r}}, t) (\mathbf{r} - \hat{\mathbf{r}}) \cdot \mathbf{N}(\mathbf{r})}{|\mathbf{r} - \hat{\mathbf{r}}|^2} d\mathcal{L}_{\hat{\mathbf{r}}}. \end{aligned} \quad (31)$$

The pertinent calculations may be found in Ref. [13].

According to Eq. (2),

$$\left( \frac{dP}{dn} \right)_b = -\frac{1}{\lambda_b} \bar{u}_n. \quad (32)$$

Eqs. (32) and (31) then imply

$$\begin{aligned} \frac{Q}{2\pi\lambda_b} \frac{\mathbf{r} \cdot \mathbf{N}}{|\mathbf{r}|^2} = \frac{1}{2} \left( \frac{1}{\lambda_a} + \frac{1}{\lambda_b} \right) \bar{u}_n(\mathbf{r}, t) \\ - \frac{1}{2\pi} \left( \frac{1}{\lambda_a} - \frac{1}{\lambda_b} \right) \int_{\mathcal{L}} \frac{\bar{u}_n(\hat{\mathbf{r}}, t) (\mathbf{r} - \hat{\mathbf{r}}) \cdot \mathbf{N}(\mathbf{r})}{|\mathbf{r} - \hat{\mathbf{r}}|^2} d\mathcal{L}_{\hat{\mathbf{r}}}. \end{aligned} \quad (33)$$

Eqs. (22), (33) fully determine the dynamics of the interface.

For the channel case (ii),

$$\begin{aligned} P = \frac{1}{2} (\rho_a + \rho_b) \mathbf{g} \cdot \mathbf{r} - \frac{1}{2} (\lambda_a^{-1} + \lambda_b^{-1}) \mathbf{u}_\infty \cdot \mathbf{r} \\ + \frac{1}{2\pi} \int_{\mathcal{L}} JG(\mathbf{r} - \hat{\mathbf{r}}) d\mathcal{L}_{\hat{\mathbf{r}}}, \end{aligned} \quad (34)$$

where

$$G(\mathbf{r} - \hat{\mathbf{r}}) = -\frac{1}{2} \ln \left[ \sin^2 \left( \frac{\pi(x - \hat{x})}{\ell} \right) + \operatorname{sh}^2 \left( \frac{\pi(y - \hat{y})}{\ell} \right) \right], \quad (35)$$

and the equation for  $\bar{u}_n(\hat{\mathbf{r}}, t)$  reads

$$\begin{aligned} \frac{1}{2} \left( \frac{1}{\lambda_a} + \frac{1}{\lambda_b} \right) \bar{u}_n(\mathbf{r}, t) \\ + \left( \frac{1}{\lambda_a} - \frac{1}{\lambda_b} \right) \frac{1}{2\pi} \int_{\mathcal{L}} \bar{u}_n(\hat{\mathbf{r}}, t) \nabla_{\mathbf{r}} G(\mathbf{r} - \hat{\mathbf{r}}) \cdot \mathbf{N}(\mathbf{r}) d\mathcal{L}_{\hat{\mathbf{r}}} \\ = \frac{1}{2} \left( \frac{1}{\lambda_a} + \frac{1}{\lambda_b} \right) u_{n,\infty}(\mathbf{r}, t) \\ + (\rho_a - \rho_b) \frac{1}{2\pi} \int_{\mathcal{L}} g_n(\hat{\mathbf{r}}, t) \nabla_{\mathbf{r}} G(\mathbf{r} - \hat{\mathbf{r}}) \cdot \mathbf{N}(\mathbf{r}) d\mathcal{L}_{\hat{\mathbf{r}}}. \end{aligned} \quad (36)$$

Here  $u_{n,\infty} = \mathbf{u}_\infty \cdot \mathbf{N}$ .

### 6. Numerical strategy

The normal advancement of the interface  $\mathbf{R} = (x(s, t), y(s, t))$  at the rate  $V_n$  is automatically ensured if one sets

$$\frac{\partial x}{\partial t} + V_s \frac{\partial x}{\partial s} = V_n \frac{\partial y}{\partial s}, \tag{37}$$

$$\frac{\partial y}{\partial t} + V_s \frac{\partial y}{\partial s} = -V_n \frac{\partial x}{\partial s}, \tag{38}$$

where  $0 < s < L(t)$ , and  $V_s, L$  are defined by Eqs. (10), (11), with  $\mathcal{K} = y_{ss}x_s - x_{ss}y_s, x_s^2 + y_s^2 = 1$ .

Eqs. (37), (38) are purely geometrical statements valid for any  $V_n$ . The interface dynamics is specified by the relation (22) where  $\bar{u}_n$  is defined by Eq. (33) or (36). Eqs. (37), (38) are considered jointly with the following periodic boundary conditions.

For the source problem,

$$\begin{aligned} x(0, t) &= x(L, t), & y(0, t) &= y(L, t), \\ x_s(0, t) &= x_s(L, t), & y_s(0, t) &= y_s(L, t). \end{aligned} \tag{39}$$

For the channel problem,

$$\begin{aligned} x(0, t) &= x(L, t) + \ell, & y(0, t) &= y(L, t), \\ x_s(0, t) &= x_s(L, t), & y_s(0, t) &= y_s(L, t). \end{aligned} \tag{40}$$

The boundary conditions should be supplemented by initial conditions,  $x_0(s) = x(s, 0), y_0(s) = y(s, 0), L_0 = L(0)$ .

The quasi-steady nature of Eqs. (33), (36) prevents evaluation of  $\bar{u}_n(s, t)$  as a solution of an initial value problem. Yet,  $\bar{u}_n(s, t)$  can be successfully calculated through the iterative procedure [21]. As the zeroth approximation one may take  $\bar{u}_n^{(0)} = Q/L_0$  for Eq. (33), and  $\bar{u}^{(0)} = u_\infty$  for Eq. (36), pertaining respectively to the undisturbed radial and rectilinear flows.

The initial configuration  $x_0(s), y_0(s)$  is conveniently given in terms of the angle  $\Theta(s)$  between the normal to the front and some fixed direction, say, the  $x$ -axis,

$$\frac{\partial x_0}{\partial s} = -\sin \Theta, \quad \frac{\partial y_0}{\partial s} = \cos \Theta. \tag{41}$$

For the source geometry we set

$$\Theta = 2\pi s/L_0 + a \sin(2\pi ns/L_0). \tag{42}$$

For the channel geometry,

$$\Theta = \pi/2 - a \cos(2\pi s/L_0). \tag{43}$$

Note that at  $a \ll 1, L_0 = \ell + O(a^2)$ .

### 7. Numerical simulations for the source geometry

In this case the system does not have an intrinsic length-scale. So  $r_{\text{ref}} = L_0/2\pi, u_{\text{ref}} = Q/r_{\text{ref}}, t_{\text{ref}} = r_{\text{ref}}/u_{\text{ref}}, D_{\text{ref}} = r_{\text{ref}}u_{\text{ref}}$  are utilized as the reference length-, velocity-, time-, and diffusivity-scale, respectively.

Fig. 1 presents results of numerical simulations for the initial condition (44) at  $\lambda_a/\lambda_b = 0.0015, D/D_{\text{ref}} = 0.001, a = 0.05, n = 6$ . A small perturbation imposed on a circular front results in a rapid development of permanently growing primary and secondary fingers. The latter are likely to undergo further

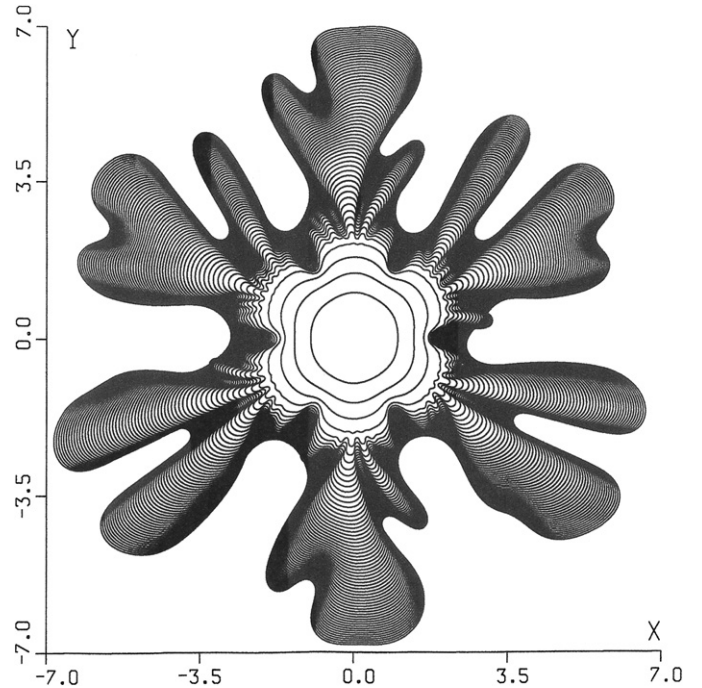


Fig. 1. Source geometry. Displacement front at several consecutive instants of time.  $\lambda_a/\lambda_b = 0.0015, D/D_{\text{ref}} = 0.001, a = 0.05, n = 6, (X, Y) = (x, y)/r_{\text{ref}}, 0 < t < 180t_{\text{ref}}$ . The time-interval between the plotted curves is set at  $3t_{\text{ref}}$ .

fractalization leading to a highly convoluted coral-like configuration. Such an intricate behavior, though perfectly in line with observations [1–3], is still rather puzzling. It has long been argued, in the context of related pattern forming systems [14–16], that the complex dynamics might be the system’s response to an ever present background (e.g. numerical) noise. In the intrinsically stable case ( $\lambda_b < \lambda_a$ ) the impact of noise is too insignificant to cause a disturbance of the advancing front. However at  $\lambda_b > \lambda_a$  the noise may play an important role of a permanently acting trigger supplying small but finite disturbances rapidly magnified by the intrinsic instability.

### 8. Numerical simulations for the channel geometry

Here the discussion is restricted to two limiting cases: (i) fingering due to viscosity contrast ( $\lambda_b > \lambda_a$ ) at  $\rho_a = \rho_b$ , and (ii) fingering due to density contrast ( $\rho_a > \rho_b$ ) at  $\lambda_a = \lambda_b$  and  $u_\infty = 0$ .

At  $\lambda_a = \lambda_b$  the integral term on the right of Eq. (36) vanishes, and one ends up with an explicit expression for  $\bar{u}_n$ , with all advantages this entails.

In the first case (i), as may be easily shown, the response of a planar interface to small harmonic perturbations ( $\sim \exp(\omega t + ikx)$ ) yields the following dispersion relation,

$$\omega = u_\infty \left( \frac{\lambda_b - \lambda_a}{\lambda_b + \lambda_a} \right) k - Dk^2. \tag{44}$$

Eq. (44) suggests the following set of the length-, time-, and velocity-scales associated with the maximum growth rate  $\omega$  of

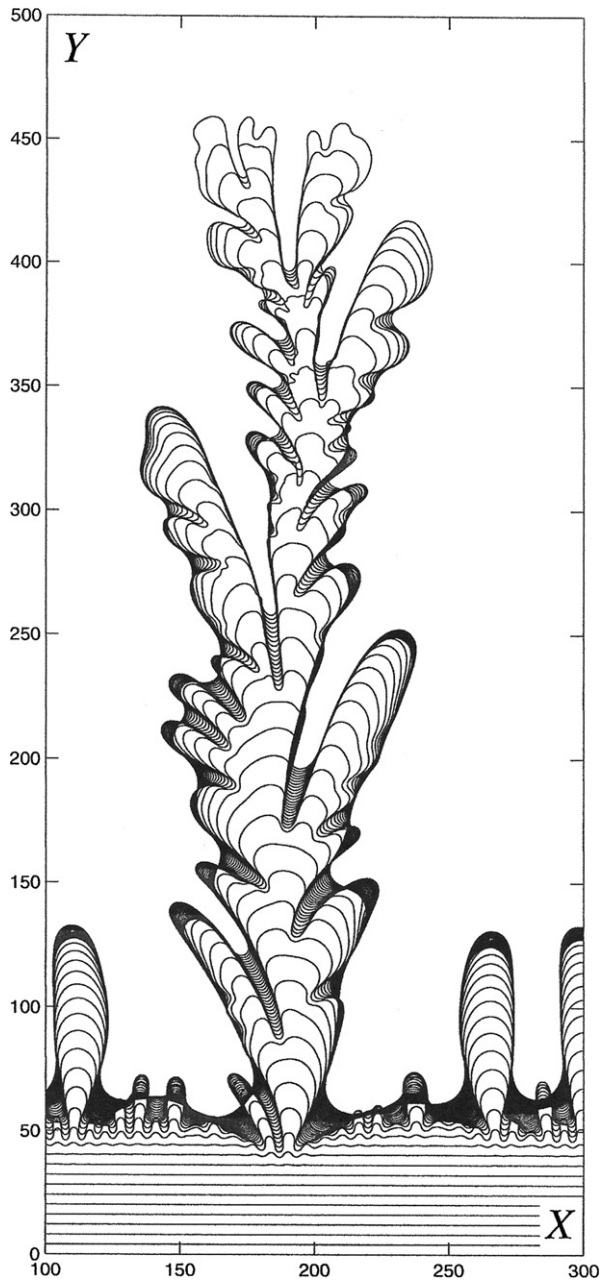


Fig. 2. Channel geometry with periodic boundary conditions. Displacement front at several consecutive instants of time;  $\rho_a = \rho_b$ ,  $\lambda_a/\lambda_b = 0.0015$ ,  $a = 0.05$ ,  $\ell = 60\pi r_{\text{ref}}$  ( $X, Y) = (x, y)/r_{\text{ref}}$ ,  $0 < t < 81t_{\text{ref}}$ . The time interval between the plotted curves is set at  $1.8t_{\text{ref}}$ .

small perturbations,

$$r_{\text{ref}} = \frac{2D}{u_{\text{ref}}} \left( \frac{\lambda_b + \lambda_a}{\lambda_b - \lambda_a} \right), \quad t_{\text{ref}} = \frac{2r_{\text{ref}}}{u_{\text{ref}}} \left( \frac{\lambda_b + \lambda_a}{\lambda_b - \lambda_a} \right), \quad (45)$$

$$u_{\text{ref}} = u_{\infty}.$$

Fig. 2 presents results of numerical simulations for initial-boundary conditions (40), (43) at  $\lambda_a/\lambda_b = 0.0015$ ,  $a = 0.05$ ,  $\ell = 60\pi r_{\text{ref}}$ . As one would anticipate, the incipient dynamics follows predictions of the linear analysis. However, with the passage of time the system undergoes ‘inverse cascade’. The development of small-scale corrugations slows down giving way to formation of a single coral-like finger. Such a behav-

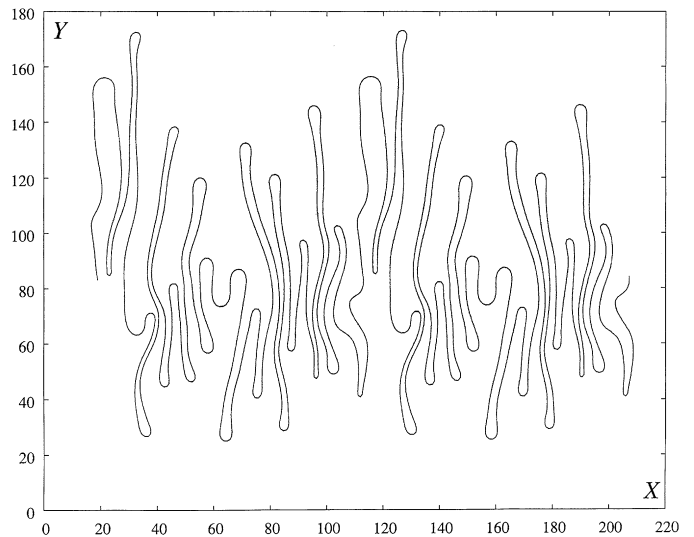


Fig. 3. Channel geometry with periodic boundary conditions.  $\rho_a > \rho_b$ ,  $\lambda_b = \lambda_a$ ,  $u_{\infty} = 0$ ,  $a = 0.05$ ,  $\ell = 30\pi r_{\text{ref}}$ , ( $X, Y) = (x, y)/r_{\text{ref}}$ . The shown configuration corresponds to  $t = 100t_{\text{ref}}$  over the doubled spatial period ( $2\ell$ ).

ior is indeed in line with experimental observations [17] and is quite common to many pattern-forming systems [4,18–20].

In the second case (ii) the dispersion relation reads

$$\omega = \frac{1}{2} \lambda g (\rho_a - \rho_b) k - Dk^2. \quad (46)$$

Here the reference scales associated with the maximum  $\omega$  are

$$r_{\text{ref}} = 2D/u_{\text{ref}}, \quad t_{\text{ref}} = 4D/u_{\text{ref}}^2, \quad (47)$$

$$u_{\text{ref}} = \lambda g (\rho_a - \rho_b) / 2.$$

Figs. 3(a) and (b) present results of numerical simulations for initial-boundary conditions (40), (43), at  $a = 0.05$  and  $\ell = 30\pi r_{\text{ref}}$ . The morphology and dynamics of fingering (meandering worms) are strikingly similar to those observed experimentally [4].

## 9. Concluding remarks

In modeling fingering instability we tried to bring into the formulation only the most essential ingredients in their simplest form. Since the instability is conditioned by the viscosity and/or density contrasts, the simplest way to elucidate their impact is through adoption of stepwise dependencies (4). This is by no means an overly drastic assumption as far as the physical understanding is concerned. In principle, in the limit of strong scale separation considered in the Letter, the problem remains perfectly tractable even when the viscosity and density vary in a continuous fashion. In this situation the hydrodynamic field acquires a finite width boundary layer along the interface. The associated mathematical problem may be tackled by the conventional machinery of matched asymptotic expansions. The emergence of the boundary layer, however, can not effect the large-scale (outer) dynamical picture, which still will be governed by Eq. (22).

Unlike the dispersion relation of the QSSA theory (Section 1), in the current study the dispersion relations (44), (46)

are time-independent, despite the unsteadiness of the basic solution. Such an outcome is clearly valid only for a limited time-period,  $t \ll t_{\text{ref}}$ . Beyond this interval the width of the inter-diffusion layer becomes comparable with that of the fingers, invalidating the concept of the scale-separation employed in the Letter.

A relation functionally similar to (22) was recently offered for the description of *immiscible* displacement [21]. However, in [21] the free-interface model is not a rigorous asymptotics extracted from the original Buckley–Leverett formulation, but rather a geometrically-invariant extrapolation from the linear analysis data [22]. A more systematic exploration of the problem produces an evolution equation distinct from (22), in which the short-wavelength dissipation is provided by the flow induced ‘stretch’ of the interface, rather than curvature. This in turn markedly affects the morphology of the developing fingers. A comparative study of the pattern forming dynamics in miscible and immiscible systems will be presented elsewhere.

### Acknowledgements

These studies were supported in part by the Alberta Research Council, the US–Israel Binational Science Foundation (Grant 2002008), the Israel Science Foundation (Grant 350/05), and the European Community Program RTN-HPRN-CT-2002-00274. Enlightening discussions with Peter Gordon, Ron Sawatzky, Mike London and Jian-Yang Yuan are gratefully acknowledged.

### References

- [1] R.J. Blackwell, J.R. Rayne, W.M. Terry, Petr. Trans. AIME 216 (1959) 1.
- [2] L. Paterson, Phys. Fluids 28 (1985) 26.
- [3] J.R. Fanchi, R.I. Christiansen, SPE 19782 (1989) 105.
- [4] R.A. Wooding, J. Fluid Mech. 39 (1969) 477.
- [5] C.T. Tan, G.M. Homsy, Phys. Fluids 29 (1986) 3549.
- [6] G.M. Homsy, Annu. Rev. Fluid Mech. 19 (1987) 271.
- [7] A. De Wit, Phys. Rev. Lett. 87 (2001) 054502.
- [8] J. Azaiez, B. Singh, Phys. Fluids 14 (2002) 1557.
- [9] C.T. Tan, G.M. Homsy, Phys. Fluids 31 (1988) 1330.
- [10] J. Yao, S. Stewart, J. Fluid Mech. 309 (1996) 225.
- [11] M. Matalon, C. Cui, J.K. Bechtold, J. Fluid Mech. 487 (2003) 179.
- [12] D.J. Struik, Lectures on Classical Differential Geometry, Dover, 1961.
- [13] N.S. Koshlyakov, E.B. Gliner, M.M. Smirnov, Differential Equations of Mathematical Physics, North-Holland, Amsterdam, 1964.
- [14] D. Bensimon, L.P. Kadanov, S. Liang, B.I. Shraiman, C. Tang, Rev. Mod. Phys. 58 (1986) 977.
- [15] D.A. Kessler, J. Koplik, H. Levine, Adv. Phys. 37 (1988) 255.
- [16] G. Joulin, P. Vidal, in: C. Godréche, P. Manneville (Eds.), Hydrodynamics and Nonlinear Instabilities, Cambridge Univ. Press, Cambridge, 1996, p. 493.
- [17] R.L. Slobod, R.A. Thomas, Soc. Pet. Eng. J. 3 (1963) 9.
- [18] P.G. Saffman, G.I. Taylor, Proc. R. Soc. London, Ser. A 245 (1958) 312.
- [19] M.Q. López-Salvans, J. Casademunt, G. Iori, F. Sagnés, Physica D 164 (2002) 127.
- [20] A. De Wit, Phys. Fluids 16 (2004) 163.
- [21] I. Brailovsky, A. Babchin, M. Frankel, G. Sivashinsky, Transp. Porous Media 63 (2006) 363.
- [22] G.I. Barenblatt, V.M. Entov, V.M. Ryzhik, Theory of Fluid Flow Through Natural Rocks, Kluwer Academic, Dordrecht, 1990.